ELSEVIER

www.elsevier.nl/locate/carres

Carbohydrate Research 328 (2000) 409–418

CARBOHYDRATE RESEARCH

Hydroxy protons in conformational study of a Lewis b tetrasaccharide derivative in aqueous solution by NMR spectroscopy

Somer Bekiroglu, Corine Sandström *, Thomas Norberg, Lennart Kenne

Department of Chemistry, Swedish University of Agricultural Sciences, PO Box 7015, SE-750 07 Uppsala, Sweden

Received 24 November 1999; accepted 9 March 2000

Abstract

The ^{1}H NMR chemical shifts, vicinal coupling constants, temperature coefficients, and exchange rates of the hydroxy protons of a Lewis b tetrasaccharide derivative, α-L-Fuc*p*-(1→2)-β-D-Gal*p*-(1→3)[α-L-Fuc*p*-(1→4)]-β-D-Glc*p*NAc-1-O$(CH_2)_2$NHCOCHCH_2, have been measured in aqueous solution. The data did not show any evidence for persistent hydrogen bonds participating in the stabilization of the structure. While most of the hydroxy proton signals have chemical shifts similar to those of the corresponding methyl glycosides, four of them, O(3)H, O(4)H, and O(6)H of Gal*p*, and O(2)H of the Fuc*p* linked to Glc*p*NAc, exhibit large upfield shifts. This shielding effect has been attributed to the orientation of the hydroxy protons toward the amphiphilic region constituted by the hydroxy groups of the Gal*p* residue and mainly the ring and methyl hydrogens of the Fuc*p* unit attached to the Glc*p*NAc. The close face to face stacking interaction between the Fuc*p* linked to the Glc*p*NAc and the Gal*p* residues, as well as the steric interaction between the Fuc*p* linked to the Gal*p* and the Glc*p*NAc are confirmed by the additional inter-residue NOEs of the exchangeable protons in sugar units which are not directly connected.

Keywords: Lewis b, tetrasaccharide; Hydroxy protons, NMR; Conformation

1. Introduction

Over the last few years, it has been shown that it is possible to observe exchangeable hydroxy protons of oligosaccharides by using water instead of D_2O as solvent. In this way, the number of NOE distance constraints used for structural and conformational information can be increased [1–8]. Moreover, measurements of coupling constants, exchange rates with water, and temperature dependence of the chemical shifts of hydroxy proton signals can provide important additional structural information in terms of hydrogen bond interactions [1–4,7–15]. We have previously reported the use of hydroxy protons in the conformational analysis of a series of disaccharides [16,17] and branched trisaccharides [7,8] in aqueous solutions. In these studies, we have shown that the NMR data obtained from hydroxy protons can be used to detect hydrogen bond interactions, to increase the number of inter-residue NOEs, and to determine the conformation around the C-5–C-6 bonds. We have also found that the chemical shifts of the hydroxy proton signals are very sensitive to the proximity of non-protonated

* Corresponding author. Fax: +46-18-673476.

0008-6215/00/$ - see front matter
PII: S0008-6215(00)00104-X

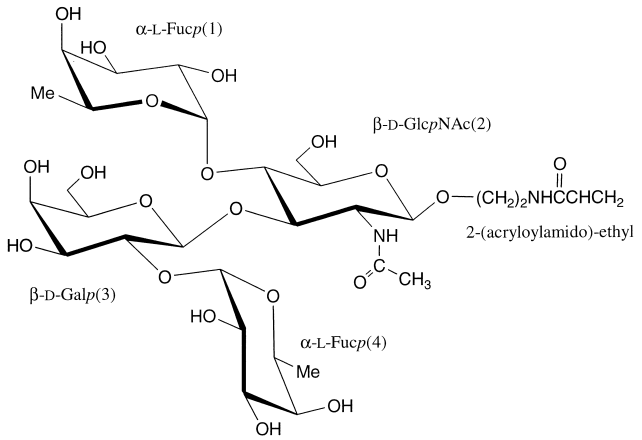

Scheme 1. Schematic representation of the Le^b tetrasaccharide derivative **1**.

oxygen atoms, and these can thereby be utilized as conformational probes for NMR studies. However, since the investigated compounds were rather flexible molecules, it was of interest to study the behaviors of hydroxy protons in a molecule with more restricted conformational freedom. For this purpose, we selected a derivative of the Lewis b (Le^b) tetrasaccharide, α-L-Fuc*p*-(1→2)-β-D-Gal*p*-(1→3)-[α-L-Fuc*p*-(1→4)]-β-D-Glc*p*NAc-1-O-$(CH_2)_2$-$NHCOCHCH_2$ (**1**), shown in Scheme 1, and designated as separately numbered residues, Fuc*p*(1)-Glc*p*NAc(2)-Gal*p*(3)-Fuc*p*(4), in the connection order. We chose this compound since, due to its biological significance, it has been widely investigated [18–26]. The structure of Le^b can also be considered as relatively rigid. Steric hindrance, hydrophobic interactions and the exo-anomeric effect contribute to its stability. The four pyranose rings are arranged to minimize steric interactions, and the two fucosyl groups are stabilized by hydrophobic contacts to either the *N*-acetylglucosamine or the galactose residue. In this work, we measured the ^1H NMR chemical shifts, vicinal coupling constants, temperature coefficients, rates of exchange with water and NOEs for the hydroxy protons of **1**, and showed that additional structural information can be obtained. This study also takes a part of a wide-scope study continuing to investigate the potential use of hydroxy protons in conformational analysis of saccharides in aqueous solution.

2. Results and discussion

Assignment of hydroxy proton resonances.— A prerequisite to detect hydroxy protons and to obtain good NMR spectra is to remove all traces of ionic impurities that can catalyze the exchange of hydroxy protons with water. It is also important to adjust the pH of the sample around neutral values in order to keep the exchange rate low. To fulfil these requirements and to observe hydroxy proton signals, the sample solution was treated with a mixed ion exchange resin [7,8]. Fig. 1 shows the one-dimensional proton NMR spectra of **1** at −10 °C, before and after treatment with Amberlite MB-3 ion exchange resin. Before the treatment with the resin (Fig. 1(a)), no signals of hydroxy protons were observed in the expected region (5–7 ppm), but after the treatment with the resin (Fig. 1(b)) the signals

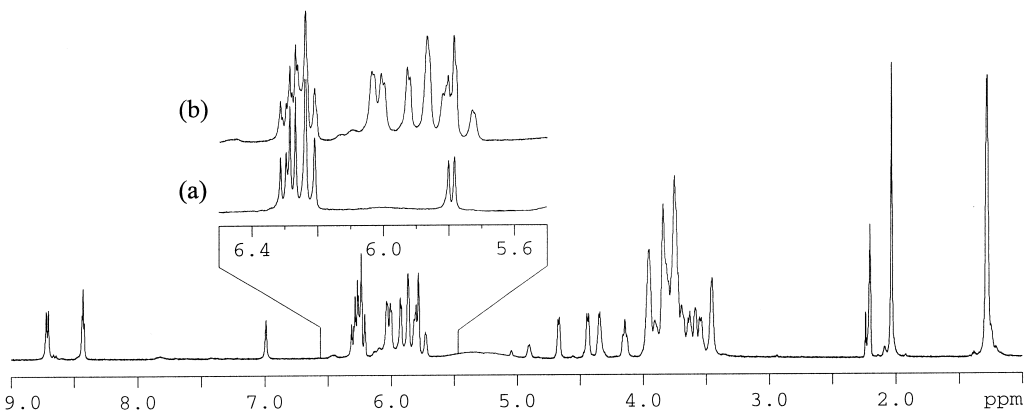

Fig. 1. One-dimensional ^1H NMR spectra (85% water–15% $(CD_3)_2CO$, −10 °C) of **1** before (a) and after (b) the treatment with the ion exchange resin.

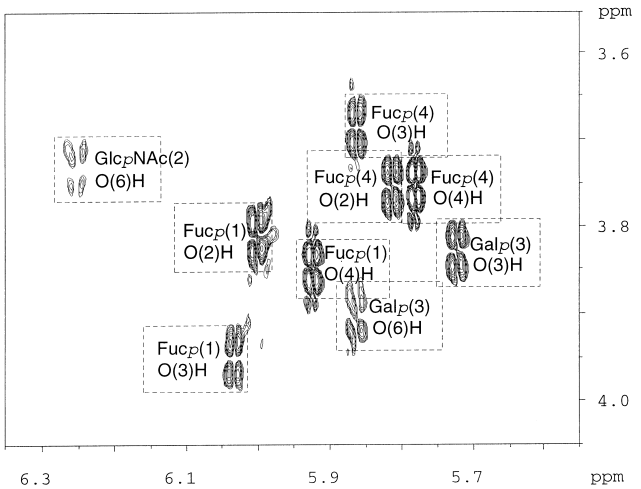

Fig. 2. Expanded region of the DQF-COSY spectra of **1** in 85% water–15% $(CD_3)_2CO$ at -10 °C, showing the scalar connectivities ($^3J_{HO,CH}$) between hydroxy and ring protons.

of the hydroxy protons could be observed as relatively narrow peaks, making their assignment on the basis of scalar connectivities to the aliphatic protons possible using COSY and TOCSY type experiments. Consequently in the region 5–7 ppm, nine cross-peaks of the hydroxy protons could be observed in the DQF-COSY spectra (Fig. 2). Although these cross-peaks were assigned to the hydroxy proton signals of Fuc*p*(1), Glc*p*NAc(2), Fuc*p*(4), and to O(3)H and O(6)H of Gal*p*(3), the O(4)H–C(4)H cross-peak of Gal*p*(3) could not be found in the DQF-COSY spectra. Inspection of the NOESY spectra (Fig. 3(b)) showed that at the chemical shift of water (5.271 ppm), there was a strong interaction with a peak at 3.841 ppm, which was assigned to C(4)H of Gal*p*(3), and thereby the resonance at 5.283 ppm could be assigned to the O(4)H signal of Gal*p*(3). No such information could be obtained from the TOCSY spectra (Fig. 3(a)), because the water stripes were masking the correlation at the resonance frequencies of protons, which are scalarly coupled to the hydroxy protons exchanging with the solvent.

The ^{1}H NMR chemical shifts (δ, ppm), chemical shift differences ($\Delta\delta$, chemical shifts of the hydroxy proton signals in the corresponding methyl monosaccharides subtracted from those in the tetrasaccharide), vicinal coupling constants ($^3J_{HO,CH}$), temperature coefficients ($d\delta/dT$), and rate of exchange with water (k_{ex}) for the hydroxy protons are listed in Table 1. The chemical shifts and coupling constants for the hydroxy proton signals of the methyl monosaccharides have been reported previously [7]. Six hydroxy protons of **1** have small $\Delta\delta$s (≤ 10.21 ppm) values indicating that their chemical shifts are very similar to those in the corresponding methyl glycosides. Four hydroxy protons, O(3)H, O(4)H, and O(6)H of Gal*p*(3), and O(2)H of Fuc*p*(4) have large negative $\Delta\delta$ values between -0.260 and -0.636 ppm.

$^3J_{HC,OH}$ coupling constants, temperature coefficients and exchange rates of hydroxy protons.—Coupling constants that do not represent conformational averaging, small temperature coefficients, and slow rate of exchange with water are indications of hydrogen

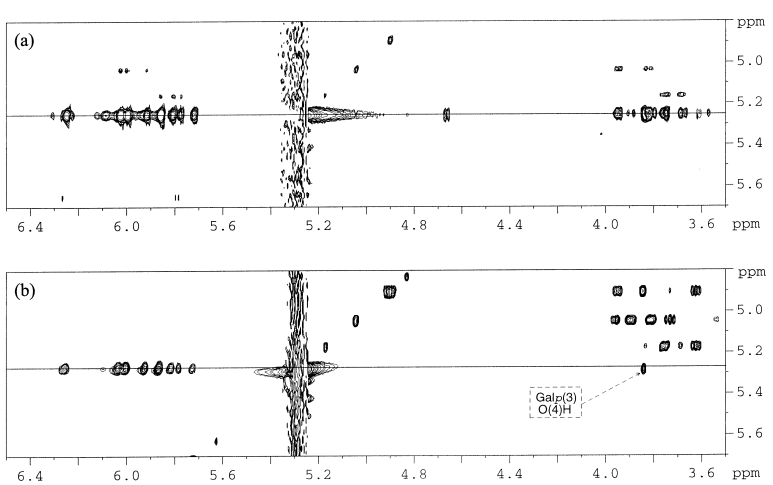

Fig. 3. Expanded region of the TOCSY (a) and NOESY (b) spectra of **1** in 85% water–15% $(CD_3)_2CO$ at -10 °C, showing the water stripe region.

Table 1
^{1}H NMR chemical shifts (δ), chemical shift differences ($\Delta\delta$), $^3J_{OH,CH}$ coupling constants (J), temperature coefficients ($d\delta/dT$), and exchange rates (k_{ex}) for the hydroxy protons of Le^b tetrasaccharide **1** in 85% water–15% $(CD_3)_2CO$ at −10 °C

		δ (ppm)	$\Delta\delta$ [a]	J (Hz)	$d\delta/dT$ (ppb deg^{-1})	k_{ex} (s^{-1})
α-L-Fuc*p*(1)	O(2)H	6.000	−0.136	6.4	−9.2	33
	O(3)H	6.033	0.103	4.8	−11.3	40
	O(4)H	5.923	−0.055	5.3	−12.3	74
β-D-Glc*p*NAc(2)	O(6)H	6.251	0.193		−11.4	
β-D-Gal*p*(3)	O(3)H	5.721	−0.401	4.8	−6.9	33
	O(4)H	5.266	−0.636		[b]	
	O(6)H	5.862	−0.260		−8.1	
α-L-Fuc*p*(4)	O(2)H	5.813	−0.323	6.8	−10.8	
	O(3)H	5.863	−0.067		−8.1	
	O(4)H	5.780	−0.198		−10.6	

[a] Chemical shift differences are calculated by subtracting the chemical shifts of the corresponding monosaccharide methyl glycosides from the chemical shifts of the hydroxy protons of **1**. Positive differences indicate downfield shift.

[b] The temperature coefficient of O(4)H of the galactose unit could not be calculated since it lies under water peak in the temperature range that could be scanned.

Low resolution of the hydroxy proton peaks and severe spectral overlap impeded the observation of the coupling constants and the calculation of the exchange rates that are not present in the table.

bonding interactions. Spectral overlap of hydroxy proton resonances, and the overlap with the water signal in the case of O(4)H of Gal*p*(3) precluded the determination of the data for all the hydroxy protons. Table 1 shows that the values of the coupling constants are all around 5.5 Hz, indicating a free rotation of the hydroxy protons around the C–O axis. The temperature coefficients ($d\delta/dT$), between −8.1 and −12.3 ppb/°C, are much larger than that expected for hydroxy protons involved in hydrogen bonding ($\leq |3|$ ppb/°C). Only O(3)H of Gal*p*(3) has a slightly smaller temperature coefficient of −6.9 ppb/°C. The exchange rates with water, which could be calculated for four hydroxy protons out of ten, have relatively similar values, indicating that no hydroxy proton is protected from exchange with the solvent through, for example, persistent hydrogen bond interactions. The exchange rates for the hydroxy protons with large $\Delta\delta$ values could not be obtained due to the signal overlap on the chemical exchange spectra except for the rate of 33 s^{-1} for O(3)H of Gal*p*(3). These data are in good agreement with previous NMR and computational studies [25,26], in which resulting structures have not suggested either direct or water-mediated hydrogen bonds in the Le^b tetrasaccharide.

Inter-residue NOEs.—A common problem in the determination of the solution conformations of oligosaccharides is the small number of inter-residue NOEs, which are usually observed between ring protons. The ten inter-residue NOEs we observed for the non-exchangeable protons in **1** are the same as those reported for the Le^b tetrasaccharide [25], indicating that the 2-(acryloylamido)-ethyl aglycone does not alter the global conformation of the molecule. Two of them, C(5)H Fuc*p*(4)–C(2)H Glc*p*NAc(2) and C(5)H Fuc*p*(1)–C(2)H Gal*p*(3), represent long-range NOEs between residues that are not directly connected. These long-range NOEs are important since, being dependent on several variable torsion angles, they are very sensitive to conformational changes. They suggest that Fuc*p*(1) and Gal*p*(3) on one hand, and Fuc*p*(4) and Glc*p*(2) on the other hand are stacked on each other. Both NOESY and ROESY spectra were recorded to discriminate between the cross-peaks that are due to dipolar relaxation and the ones due to chemical exchange. No cross-peaks were observed between hydroxy protons, but 22 intra- and five inter-residue cross-peaks due to dipolar relaxation could be observed between hydroxy protons and ring protons (Table 2). The inter-residue NOEs are O(3)H Gal*p*(3)–C(1)H

Fuc*p*(4), O(4)H Gal*p*(3)–C(5)H Fuc*p*(1), O(4)H Gal*p*(3)–C(3)H Fuc*p*(1), O(4)H Gal*p*(3)–C(1)H Glc*p*NAc(2), and O(6)H Gal*p*(3)–C(5)H Glc*p*NAc(2). Three inter-residue NOEs could also be detected between the amide proton of the NAc group on Glc*p*NAc(2) and C(1)H of Gal*p*(3), C(5)H and the C(6)H of Fuc*p*(4). Together with these inter-residue NOEs, the five intra-residue NOEs of the same amide proton are also listed in Table 2. Although the magnitude of the NOEs detected between the amide proton of the NAc group on Glc*p*NAc(2) and C(5)H and the C(6)H of Fuc*p*(4) are smaller than the NOE of C(1)H of Gal*p*(3), these NOEs reinforce the sole NOE between C(2)H of Glc*p*NAc(2) and C(5)H of Fuc*p*(4), being used to verify the contact between Glc*p*NAc(2) and Fuc*p*(4). Finally, when the present NMR and conformational data concerning the exchangeable proton resonances are taken into consideration, it is seen that the two previously investigated stacking interactions, Fuc*p*(1)/Gal*p*(3) and Glc*p*NAc(2)/Fuc*p*(4), and the rigid backbone structure determined by the glycosidic torsions are confirmed by these additional NOEs observed for the exchangeable protons on **1**.

Interpretation of hydroxy proton chemical shifts.—The chemical shifts of hydroxy proton signals are subject to several intrinsic effects, which have been difficult to predict so far. However, all the present structure elucidation techniques based on chemical shift susceptibilities are functions depicting these factors in a correlation with the structural information. In our previous studies on disaccharides [16,17] and trisaccharides [8], we found that the chemical shifts of hydroxy proton signals were sensitive to the proximity between the hydroxy proton and other oxygen atoms. Large upfield shifts were observed for signals of hydroxy protons close to non-protonated oxygens with the largest shifts observed for hydroxy protons being close to O(5) oxygens. On the contrary, hydroxy protons which were only close to other hydroxy groups or to the oxygen of their own glycosidic linkage had small $\Delta\delta$ values.

According to the resulting structure from the MM3 calculations (Figs. 4 and 5), distance measurements between hydroxy protons having large $\Delta\delta$s and non-protonated oxygens which may cause the upfield shifts showed that, excluding their own ring oxygen O(5), the O(3)H, O(4)H, and O(6)H of Gal*p*(3), and

Table 2
NOEs detected for the exchangeable protons of the Le[b] tetrasaccharide part of **1**

Lewis b tetrasaccharide					
Exchangeable proton	Int(ra/er) [a]-residue NOEs	Exchangeable proton	Int(ra/er) [a]-residue NOEs	Exchangeable proton	Int(ra/er) [a]-residue NOEs
NHAc (2)	*H1* (*3*)	O(3)H (1)	H3		*H5* (*1*)
	H5, *Me*(*4*)		H4		*H1* (*2*)
	H1				
	H2	O(4)H (1)	H3	O(6)H (3)	H6a, H6b
	H3		H4		*H5* (*2*)
	H5		H5		
	Me(NAc)		Me	O(2)H (4)	H1
					H2
O(6)H (2)	H6a, H6b	O(3)H (3)	H2		
			H3	O(3)H (4)	H2
O(2)H (1)	H1		*H1* (*4*)		H3
	H2				
	H3	O(4)H (3)	H2	O(4)H (4)	H4
			H4		H5
			H3 (*1*)		Me

[a] The inter-residue NOEs are shown in italic whereas intra-residue NOEs are in plain text.

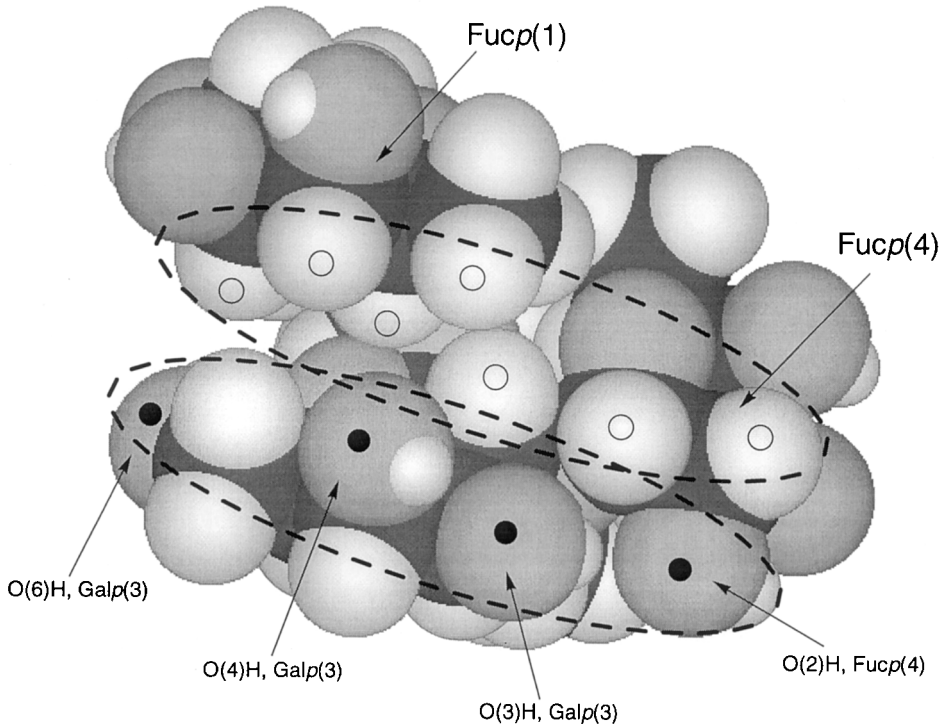

Fig. 4. Space filling model of the energetically best structure of the MM3 calculations on **1**. The dashed ellipses show hydrophilic and hydrophobic sides of Fuc*p*(1) and Gal*p*(3), respectively. The hydrogens that are designated with circles and hydroxy groups that are designated with filled circles constitute the two faces creating the amphiphilic region.

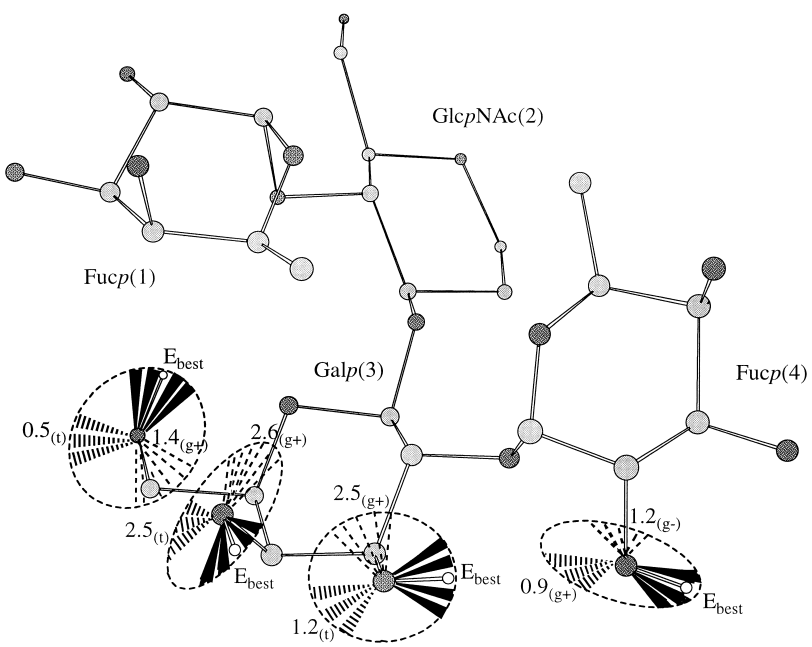

Fig. 5. A picture of Le^b tetrasaccharide as seen from the Fuc*p*(1)–Gal*p*(3)–Fuc*p*(4) face of the tetrasaccharide. The elliptic circles designate the rotational orbits of each hydroxy proton. The orbits are divided into three major staggered conformational areas as gauche (−), gauche (+), and trans. These conformations are defined with respect to the torsions, C(5)–C(6)–O(6)–O(6)H, C(3)–C(4)–O(4)–O(4)H, and C(2)–C(3)–O(3)–O(3)H on Gal*p*(3) and C(1)–C(2)–O(2)–O(2)H on Fuc*p*(4). The energies of each conformer are indicated with stripes of different intensity and represented by only one conformational data point of energy calculations. Each conformation has an energy value in kcal mol^{-1}, which represents the lowest energy that could be achieved with that conformation of the hydroxy proton, regardless of the rest of the structure. The aglycone and NAc substituents on Glc*p*NAc, as well as unessential hydrogens were omitted for simplicity.

O(2)H of Fuc*p*(4) did not result in sufficient proximities (< 2.5 Å), even if they are deliberately directed. Furthermore, the conformations of O(3)H and O(4)H of Gal*p*(3), when they are in the closest positions to the non-protonated oxygens, require rather high energy (Fig. 5) to intrude into the sterically crowded region between Fuc*p*(1) and Gal*p*(3). Additionally, in the case of O(3)H of Gal*p*(3) and the O(2)H of Fuc*p*(4), which are only close to their own glycosidic linkage oxygen, we see that they also have large $\Delta\delta$s, which should normally be small [8,16,17]. One argument supporting our conventional explanation for large negative $\Delta\delta$s could be that the lone pairs of hydroxy group oxygens in rigid molecules can have more restricted orientations, causing an upfield shift for the hydroxy proton signals to which they are close in space.

An alternative explanation for the chemical shifts of the hydroxy protons can be found in their orientation relative to the hydrophobic/hydrophilic faces of the tetrasaccharide [23]. Figs. 4 and 5 and Table 1 show that the hydroxy protons that are located at the surface of the tetrasaccharide and that are most exposed to the bulk water without any perturbed water network of amphiphilic regions have small $\Delta\delta$s. Their interaction with the bulk water is very similar to that in the monosaccharides, and accordingly so are their chemical shifts. Consequently, examination of the positions of the hydroxy groups having large $\Delta\delta$s indicates that they are all placed in the vicinity of the amphiphilic regions constituted by primarily the hydrophobic face of Fuc*p*(1) and the hydrophilic face of Gal*p*(3). More specifically, O(4)H ($\Delta\delta = -0.636$ ppm) and O(3)H ($\Delta\delta = -0.401$ ppm) of Gal*p*(3), which are located under the hydrophobic face of Fuc*p*(1), experience large upfield shifts. The O(2)H of Fuc*p*(4) and O(6)H of Gal*p*(3) sitting on the two far sides of the amphiphilic region are also influenced by this effect. However, the extent of the chemical shift change is less pronounced for O(2)H of Fuc*p*(4) and O(6)H of Gal*p*(3), showing smaller $\Delta\delta$ values, -0.323 and -0.260 ppm respectively, than O(4)H and O(3)H of Gal*p*(3). In Fig. 4, these hydroxy groups can be seen as a belt covering the hydrophobic side of Fuc*p*(1). In addition to their peculiar $\Delta\delta$ values, it is also of interest to note that they participate in either primary or secondary key polar interactions observed in the protein binding studies [23], which bear the indications for the perturbed water molecules [24] providing the conditions for molecular recognition in aqueous solution.

3. Conclusions

The NMR data obtained for the hydroxy protons of the tetrasaccharide derivative **1** do not indicate any inter-residue hydrogen bonds in water solutions. The NOEs observed for O(4)H of Gal*p*(3) support the location of Fuc*p*(1) placed on the hydrophilic face of Gal*p*(3). A similar kind of steric interaction between Fuc*p*(4) and Glc*p*NAc(2) is confirmed by the NOEs detected for the amide proton on the NAc group of Glc*p*NAc(2).

The upfield shifts for the hydroxy proton signals have tentatively been explained on the basis of hydrophobic/hydrophilic interactions. The hydroxy protons, O(3)H, O(4)H, and O(6)H of Gal*p*(3) and O(2)H of Fuc*p*(4), which are situated around the hydrophobic strand composed of mainly H(3), H(4), H(5), and methyl group of Fuc*p*(1) experience upfield shifts. As amphiphilic regions create perturbed water behavior due to both hydrophilic and hydrophobic properties, being close to a hydrophobic strand, as defined above, together with the hydrophilic counterpart, which is indeed constituted by the hydroxy groups themselves, can result in a disturbed solvent–solute interaction. This perturbation on the solvent behavior could be the reason for the upfield shifts through the interruption of the strong hydrogen bonding network of water with the hydroxy groups. On the other hand, the hydroxy protons that are located at the surface of the tetrasaccharide and that are most exposed to the bulk water have chemical shifts similar to those in the corresponding methyl glycosides. Considering the previous correlation between such an upfield shift of the hydroxy protons and their proximity to non-protonated oxygens, this study provides an alternative explanation for the same effect. In fact, the reason for the upfield shifts due to

differences in hydrogen bonding strengths could be the same in all the studied molecules encountering perturbed water molecules around the hydroxy protons, which in turn show large negative $\Delta\delta$ values. Therefore more experimental and theoretical data on hydroxy proton chemical shifts in rigid saccharides would be appreciated in order to be able to conclude decisively about the origin of the upfield shifts measured and to use it as a conformational probe in a more quantitative manner for structural and possibly binding studies of hydroxy groups. Our computational studies pursuing clarification on the perturbed water interactions with solute molecules are continuing.

4. Experimental

The synthesis of the Lewis b derivative **1** has been described elsewhere [27].

Sample preparation for NMR studies.—The NMR sample tube was soaked for more than 1 h in a 50 mM solution of phosphate buffer (pH 7) to minimize adsorption of impurities from glassware [11]. The Le^b tetrasaccharide derivative was purified on an Amberlite MB-3 mixed ion-exchange resin prior to NMR experiments. The batch method, addition of the resin directly into the sample, followed by stirring, was used to treat the aqueous sample with Amberlite MB-3 in a plastic tube. The treated sample was then taken out with a syringe into another tube, whose content was finally lyophilized and used for the NMR sample preparation.

NMR spectroscopy.—All NMR experiments were performed on a Bruker DRX-600 spectrometer operating at 600.13 MHz for proton observation. The tetrasaccharide was dissolved in a mixture of 85% water–15% $(CD_3)_2CO$ (0.2 mL) to give a sample concentration of ca. 5 mM. The addition of acetone to the samples allowed lowering of the sample temperature to -12 °C without freezing. All spectra unless specified were recorded at -10 °C except for the temperature coefficients, which were measured by variation of the temperature from -10 to 20 °C in 5 °C steps. The ^{1}H NMR spectra were referenced by setting the residual acetone-d_5 signal to $\delta_H = 2.204$ ppm. One- and two-dimensional ^{1}H NMR spectra were acquired using the WATERGATE pulse sequence [28] for suppression of the water signal. The 2D NMR spectra were recorded in the phase-sensitive mode using the TPPI method [29]. NOESY and ROESY spectra were recorded with mixing times (τ_m) of 50 and 100 ms with 512 spectra of 4 K data points. For each FID, 80 scans were recorded using a repetition delay of 2 s. The data were zero-filled to 2×1 K before applying a $\pi/2$ shifted sine-square bell window function in both dimensions. The rates of exchange of the hydroxy protons with water were calculated from 2D phase-sensitive chemical exchange experiments. Mixing times of 3–18 ms in steps of 3 ms were used. 128 FIDs of 2 K data points were acquired and a recycle delay of 1.5 s was used. A polynomial baseline correction was applied in both dimensions. The volumes of the NOE cross-peaks and diagonal peaks were measured using the program AURELIA (Bruker, Germany). The exchange rate constants were calculated as the ratio of the initial build-up rates of the exchange peaks over the volume of the diagonal peaks at zero mixing time. ^{1}H and ^{13}C chemical shifts are available as supplementary material from the correspondence author.

MM3 calculations.—The aglycone was substituted with –OMe instead of the 2-(acryloylamido)-ethyl aglycone part of **1** since it did not effect the structure as validated by the same NOE pattern observed and very minor differences in chemical shifts for the non-exchangeable protons. Depending on the exo-anomeric effect and the fact that the aglycone would point away from Glc*p*NAc(2), the –OMe group was placed with the $\phi_{C(1)H-C(1)-O(x)-C(x)}$ angle 60°. The conformation of the acetamido substituent of Glc*p*NAc(2) on the other hand was determined to be anti for the amido proton and C(2)H of Glc*p*NAc(2) because of their large coupling constant, $^3J_{HN,C(2)H} = 10.1$, and of the strong NOE observed between the methyl protons on the acetamido group and the C(1)H of Gal*p* (3) and the C(1)H, C(3)H of Glc*p*NAc(2).

In modeling, we also made use of the glycosidic dihedral angles (ϕ = C(1)H–C(1)–O(x)–

C(x) and ψ = C(1)–O(x)–C(x)–C(x)H) previously reported [25,26], where our experimental data fit the resulting structures. This would be already expected due to the rigid structures of Lewis oligosaccharides. To be statistically coherent an average of each glycosidic torsion angle pair was used, and they resulted in the values ϕ/ψ 9°/24.5° of Fuc*p*(1)–Glc*p*NAc(2), $\phi/\psi = 49°/25°$ of Gal*p*(3)–Glc*p*NAc(2), and $\phi/\psi = 43.5°/23°$ of Fuc*p*(4)–Gal*p*(3). Apart from the glycosidic torsion angles that were imposed, the approximation that allows pyranose ring conformations to be described by two torsional degrees of freedom per residue [30] was employed next to construct eight different clockwise and counter-clockwise conformations on residues (1), (3) and (4). Then the conformations around O(5)–C(5)–C(6)–O(6), (ω), and C(5)–C(6)–O(6)–O(6)H, (ω(H)) dihedrals of Glc*p*NAc(2) and Gal*p*(3) were searched in a four-dimensional grid search manner with a step size of 120°, visiting gauche (+), gauche (−) and trans conformers. Finally all input geometries were used to make a three-dimensional grid search again with a step size of 120°, which takes gauche (+), gauche (−) and trans conformations into account for the dihedrals of C(3)–C(4)–O(4)–O(4)H and C(2)–C(3)–O(3)–O(3)H on Gal*p*(3) and C(1)–C(2)–O(2)–O(2)H on Fuc*p*(4), which will be addressed later as O(4)H and O(3)H torsions on Gal*p*(3) and O(2)H torsion on Fuc*p*(4), respectively. To do this, we first set the O(2)H torsion of Fuc*p*(4) to gauche (+), gauche (−) and trans conformations. By using the dihedral angle driver option allowing us to set each rigid rotation from the initial geometry, followed by a full energy minimization, the resulting 1944 input structures were then run with a 3×3 grid search on O(4)H and O(3) of Gal*p*(3) torsions.

All calculations were performed on a SGI Octane R10000 workstation using the molecular mechanics program MM3 [31], which has been widely used for carbohydrates. The MM3 program has also been shown to be suitable for correct calculations of ring geometries and glycosidic torsion angles of saccharides [32,33]. Moreover, in order to apply a more realistic approach than fixing the angle rigidly for each dihedral to be checked, it is also convenient to optimize geometries fully at each point of the conformational grid search. The dielectric constant was kept at 4 and a block diagonal minimization method was applied to all calculations using the default convergence criteria, which initially becomes $0.00003\sqrt{n}$ Å for average movement (n = number of atom) and switches to an energy change of $0.00008*n$ kcal mol^{-1} per five iterations, if the first criterion is not satisfied.

In the end, the energetically best structure had the overall steric energy of 44.4362 kcal mol^{-1} and the so-called CAC conformation for hydroxy groups, designating clockwise for Fuc*p*(1), counter-clockwise for Gal*p*(3) and clockwise for Fuc*p*(4), respectively. The glycosidic torsions for the best structure were found to be $\phi/\psi = 40°/24°$ of Fuc*p*(1)–Glc*p*NAc(2), $\phi/\psi = 48°/23°$ of Gal*p*(3)–Glc*p*NAc(2), and $\phi/\psi = 38°/20°$ of Fuc*p*(4)–Gal*p*(3), which only differ by $\leq 5.5°$ from the initial values. The values measured on the best structure for the angles ω of Glc*p*NAc(2) and Gal*p*(3) were 60 and 64°, while ω(H) of the same residues were −62 and −63°, respectively. However, this energetically best conformation does not supply a general view in terms of dynamic changes especially for the exocyclic substituents. Therefore we processed the data so that it became possible to visualize the rotations around the torsions O(3)H, and O(3)H of Gal*p*(3) and O(2)H of Fuc*p*(4) (Fig. 5). Each conformational energy for each staggered conformation was chosen to be the best energy conformer of that hydroxy group regardless of the rest of the structure. That is the energy differences do not show the isolated energies of each conformer at a certain conformation of the whole structure.

The 3D structure and space-filling model of **1** were made using the CS Chem Draw Pro and Chem3D Pro version 4.0.

Acknowledgements

This work was supported by grants from the Swedish Natural Research Council and CARENET-2.

References

[1] L. Poppe, H. van Halbeek, *J. Am. Chem. Soc.*, 113 (1991) 363–365.
[2] H. van Halbeek, L. Poppe, *Magn. Reson. Chem.*, 30 (1992) S74–S86.
[3] L. Poppe, R. Stuike-Prill, B. Meyer, H. van Halbeek, *J. Biomol. NMR*, 2 (1992) 109–136.
[4] L. Poppe, H. van Halbeek, *J. Am. Chem. Soc.*, 114 (1992) 1092–1094.
[5] J.R. Brisson, S. Uhrinova, R.J. Woods, M. van der Zwan, H.C. Jarrell, L.C. Paoletti, D.L. Kasper, H.J. Jennings, *Biochemistry*, 36 (1997) 3278–3292.
[6] R. Harris, T.J. Rutherford, M.J. Milton, S.W. Homans, *J. Biomol. NMR*, 9 (1997) 47–54.
[7] C. Sandström, H. Baumann, L. Kenne, *J. Chem. Soc. Perkin Trans. 2*, (1998) 809–815.
[8] C. Sandström, H. Baumann, L. Kenne, *J. Chem. Soc. Perkin Trans. 2*, (1998) 2385–2393.
[9] L. Poppe, H. van Halbeek, *Nat. Struct. Biol.*, 1 (1994) 215–216.
[10] S.Q. Sheng, H. van Halbeek, *Biochem. Biophys. Res. Commun.*, 215 (1995) 504–510.
[11] B. Adams, L. Lerner, *J. Am. Chem. Soc.*, 114 (1992) 4827–4829.
[12] B.R. Leeflang, J.F.G. Vliegenthart, L.M.J. Kroon-Batenburg, B.P. van Eijck, J. Kroon, *Carbohydr. Res.*, 230 (1992) 41–61.
[13] D.R. Bundle, H. Baumann, J.R. Brisson, S.M. Gagné, A. Zdanov, M. Cygler, *Biochemistry*, 33 (1994) 5183–5192.
[14] B. Adams, L.E. Lerner, *Magn. Reson. Chem.*, 32 (1994) 225–230.
[15] S.Q. Sheng, R. Cherniak, H. van Halbeek, *Anal. Biochem.*, 256 (1998) 63–66.
[16] C. Sandström, G. Magnusson, U. Nilsson, L. Kenne, *Carbohydr. Res.*, 322 (1999) 46–56.
[17] I. Ivarsson, C. Sandström, L. Kenne, unpublished results.
[18] R.U. Lemieux, *Chem. Soc. Rev.*, 7 (1978) 423–452.
[19] R.U. Lemieux, K. Bock, L.T.J. Delbaere, S. Koto, V.S. Rao, *Can. J. Chem.*, 58 (1980) 631–653.
[20] O. Hindsgaul, T. Norberg, J. Le Pendu, R.U. Lemieux, *Carbohydr. Res.*, 109 (1982) 109–142.
[21] R.U. Lemieux, K. Bock, *Arch. Biochem. Biophys.*, 221 (1983) 125–134.
[22] U. Spohr, R.U. Lemieux, *Carbohydr. Res.*, 174 (1988) 211–237.
[23] R.U. Lemieux, *Chem. Soc. Rev.*, 18 (1989) 347–374.
[24] R.U. Lemieux, *Acc. Chem. Res.*, 29 (1996) 373–380.
[25] A. Geyer, G. Hummel, T. Eisele, S. Reinhardt, R.R. Schmidt, *Chem. Eur. J.*, 2 (1996) 981–988.
[26] A. Imberty, E. Mikros, J. Koca, R. Mollicone, R. Oriol, S. Perez, *Glycoconjugate J.*, 12 (1995) 331–349.
[27] K. Eklind, R. Gustafsson, A.K. Tiden, T. Norberg, P.M. Åberg, *J. Carbohydr. Chem.*, 15 (1996) 1161–1178.
[28] M. Piotto, V. Saudek, V. Sklenár, *J. Biomol. NMR*, 2 (1992) 661.
[29] D. Marion, K. Wüthrich, *Biochem. Biophys. Res. Commun.*, 113 (1983) 967.
[30] S.N. Ha, L.J. Madsen, J.W. Brady, *Biopolymers*, 27 (1988) 1922–1952.
[31] MM3(1996), Department of Chemistry, University of Georgia, Athens, GA 30602, USA.
[32] S. Perez, A. Imberty, J.P. Carver, *Adv. Comput. Biol.*, 1 (1994) 146–202.
[33] A.D. French, M.K. Dowd, *J. Mol. Struct.* (*Theochem.*), 286 (1993) 183–201.